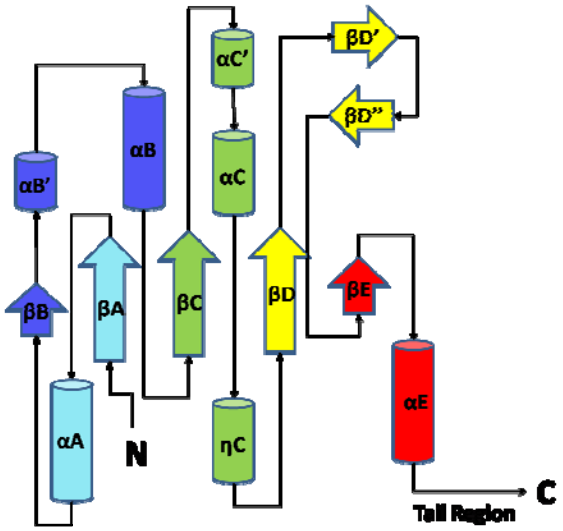

Figure S1. Topology diagram of the protein fold of BcSEFIR. The α- and 3_{10}-helices are represented by cylinders and β-strands are represented by arrows. Secondary structure elements are labeled.

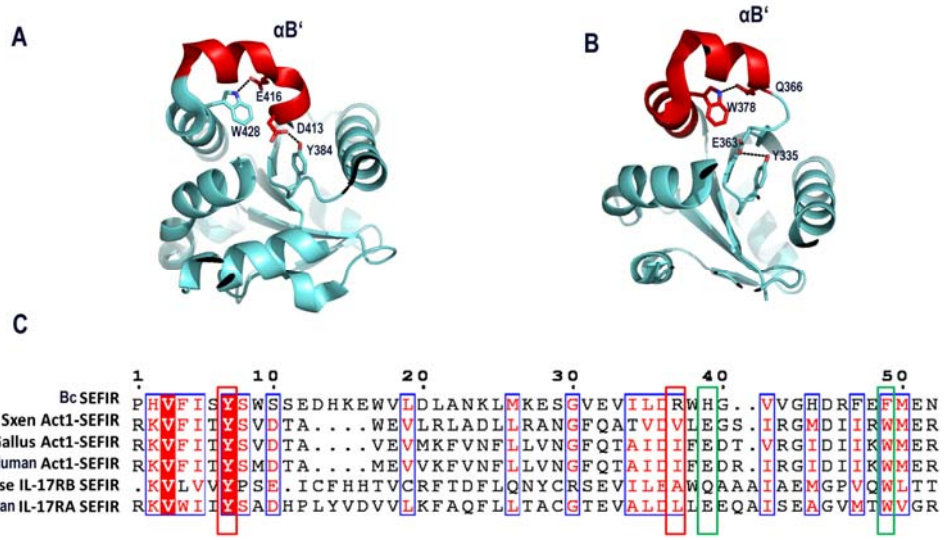

Figure S2. The helix αB' in SEFIRs are hydrogen bond to helix αB. IL-17RA-SEFIR helix αB', hydrophobic interactions and hydrogen bond are shown. (B) IL-17RB-SEFIR helix αB', hydrophobic interactions and hydrogen bond are shown. (C) Multiple sequence alignment of selected SEFIR domains, the conserved residues which formed hydrogen bond are shown.

SEFIR domain form Bacillus cereus, Xenopus (Silurana) tropicalis, Gallus, human Act1 and mouse IL-17RB-SEFIR, human IL-17RA-SEFIR are used in the alignment.

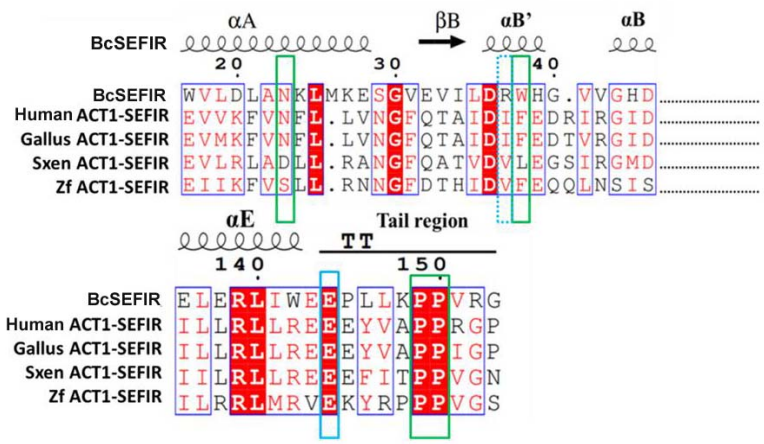

Figure S3. Multiple sequence alignment of BcSEFIR and Act1-SEFIR in different species. SEFIR domain form *Bacillus cereus*, Act1-SEFIR domain from human, Gallus, Xenopus (Silurana) tropicalis and Zebra fish are used in the alignment.

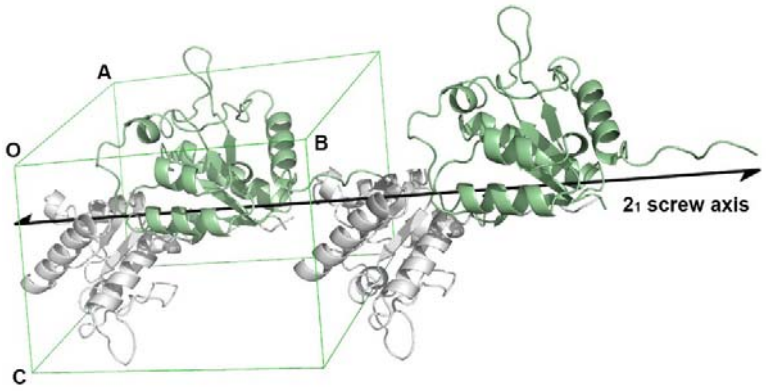

Figure S4. Assembly of theBcSEFIRinto higher order oligomers. Via the asymmetric association between two adjacent BcSEFIR molecules, a fiber-like oligomeric structure with 2_1 screw axis is formed in the crystal, which could be a plausible model of SEFIR-mediated signaling.

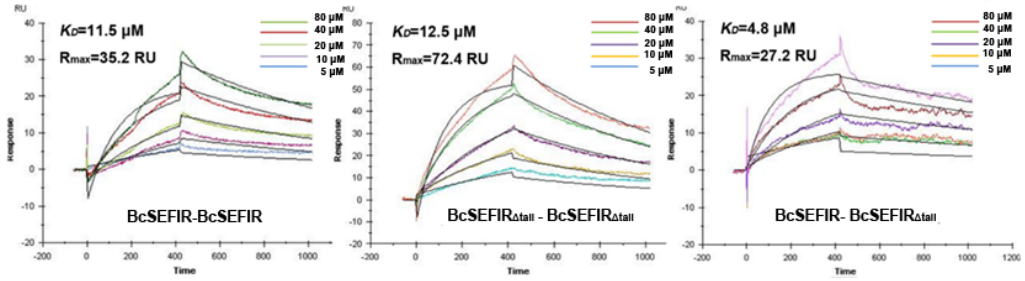

Figure S5. SPR Binding assay of BcSEFIR. Five different concentations of ligand BcSEFIR were injected over the surface to which was immobilized with BcSEFIR proteins. The binding affinities between BcSEFIR-BcSEFIR, BcSEFIR$_{\Delta tail}$-BcSEFIR$_{\Delta tail}$， BcSEFIR-BcSEFIR$_{\Delta tail}$ were all assessed.

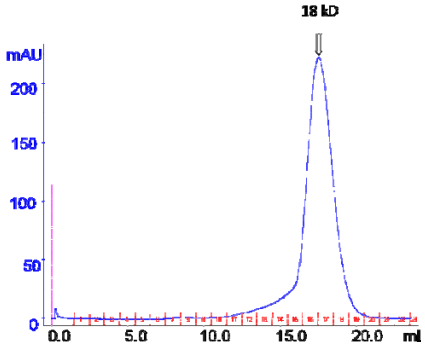

Figure S6. Gel filtration chromatography profile of the recombinant BcSEFIR. BcSEFIR was eluted as monomer in solution using size exclusion chromatography, arrow at the top indicate the eluted position of the molecular weight.

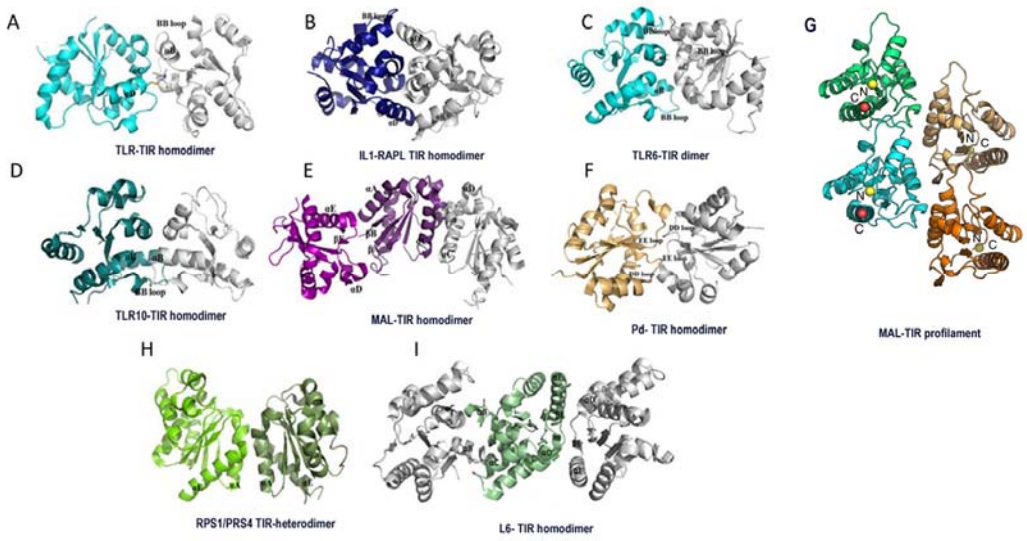

Figure S7. Homodimerization of TIR domains in different species. A number of homotypic TIR domain complexes have been proposed, but no common surface has been identified in mammalian TIR domains. A conserved symmetric TIR-TIR domain interface has been observed in the crystal structures of the bacterial TIR domains from PdTIR and TcpB, which share more than 60 % sequence identify. As to R protein RPS4, RRS1 and AtTIR in Arabidopsis, they all reveal a common TIR-TIR domain interface, while flax R-protein L6 revealed totally different interfaces.

Table S1.Crystal lattice contacts identified by the PISA (Protein Interfaces, Surfaces, and Assemblies) server.

BcSEFIR	Interface area	Number of hydrogen bond	Number of salt bridge
asymmetric interface	662 Å^2	5	10
interface 1	166 Å^2	1	0
interface 2	146 Å^2	5	0

BcSEFIR$_{\Delta tail}$	Interface area	Number of hydrogen bond	Number of salt bridge
symmetric interface	958 Å^2	9	5
interface 1	512 Å^2	3	2
interface 2	263 Å^2	1	2
interface 3	227 Å^2	1	2
interface 4	193.9 Å^2	1	0
Interface 5	153 Å^2	1	3